Effects of background noises on nonlinear dynamics of a modelled thermoacoustic combustor

Xinyan Li,[1] Dan Zhao,[2,a)] and Xuan Li[3]

[1]*School of Mechanical and Aerospace Engineering, College of Engineering, Nanyang Technological University, 50 Nanyang Avenue, Singapore 639798, Singapore*

[2]*Department of Mechanical Engineering, College of Engineering, University of Canterbury, Private Bag 4800, Christchurch 8140, New Zealand*

[3]*China Aerospace Science and Industry Corporation, Yungang West No. 1, Fengtai, Beijing 100074, China*

In this work, the effects of background noises on nonlinear dynamics of a modelled standing-wave thermoacoustic system with subcritical Hopf bifurcation behaviors are studied. These noises include (1) pressure-coupled (acoustic), (2) velocity-coupled (flow), and (3) external combustion noise. It is found that these three types of background noises play important, but different roles in changing the hysteresis width and stability boundary. In addition, the stochastic transition from stability to instability is investigated, as the noise intensity is varied. Two different stochastic P-bifurcations are identified. One is related to a craterlike probability density distribution. The other is associated with a probability density distribution characterized with two peaks and one trough. With each type of noise affecting the system's stochastic behaviors being evaluated, the effect of two different types of noises is then studied. It is shown that the combined noises (types 1 and 2) cannot only destabilize global stable thermoacoustic system, but also stabilize linearly unstable system. This depends strongly on the superimposition form of the two types of noises. In addition, when the thermoacoustic system is disturbed by the combined noise (types 3 and 1 or types 3 and 2), the transition process is dominated by the combustion noise.
© 2018 Acoustical Society of America. https://doi.org/10.1121/1.5020059

I. INTRODUCTION

Self-sustained thermoacoustic instabilities may occur in different types of propulsion systems, such as liquid-fuel/solid rocket motors, aero-engines, and augmenters. Such instabilities also take place in land-based industrial gas turbines,[1] furnaces, and boilers. In order to meet the increasingly stringent requirement of low NOx emission, lean-premixed prevaporized techniques are preferred in industrial combustion systems. This combustion technology makes the industrial combustors more susceptible to thermoacoustic instabilities. Thus, thermoacoustic oscillations occur more frequently in the new generation of gas turbines and aero-engines. Thermoacoustic instabilities are typically characterized by large-amplitude pressure or velocity oscillations. It is generally caused[2] by the dynamic coupling process between unsteady heat release and acoustic disturbances. Unsteady combustion responds dynamically to oncoming acoustic waves, which propagate within the combustor. To describe the coupling, Rayleigh[3] proposed a well-known criterion, which reveals the generation mechanism of thermoacoustic instabilities. It is stated that when the unsteady heat release and the acoustic pressure are in phase, the acoustic wave will gain energy from the heat source. Moreover, if the energy gained from the heat source exceeds the acoustic loss due to acoustic damping, the small amplitude acoustic perturbation will grow into large-amplitude limit cycle oscillations. Such oscillations are known as thermoacoustic instabilities.

Large-amplitude limit cycle oscillations may lead to many unwanted outcomes, such as unacceptable noise and structural vibrations. It may also lead to overheating and high-cycle mechanical fatigue problems. In order to eliminate the unfavorable thermoacoustic oscillations, two main approaches are proposed and tested. One is passive control[4,5] and the other is active control. To design a stable combustor and to prevent the onset of such damaging oscillations, an accurate prediction of stability boundary and behaviors of a given combustion system is needed. Two main approaches are generally used to study the stability of thermoacoustic system, linear modal analysis and nonlinear analysis. Conventional modal analysis can provide insightful information about the growth rate and eigen-frequency of thermoacoustic modes. This information is important for acoustic dampers' design. However, it cannot predict the amplitude of self-excited thermoacoustic oscillations. In addition, such modal analysis fails to predict the instability, if the thermoacoustic system is in the hysteresis loop, where a stable status and a stable limit cycle coexist. Hysteresis is a typical characteristic of subcritical Hopf bifurcations. In fact, thermoacoustic systems can lose stability via a subcritical[6] or supercritical bifurcation,[7,8] which depends strongly on the specific operation condition.[9] Compared with supercritical Hopf bifurcation, subcritical bifurcation is more damaging to

a)Electronic mail: dan.zhao@canterbury.ac.nz

the combustor, as a sudden transition to large amplitude oscillations may occur, due to a small change in some important system parameters, such as (1) heating power,[10] (2) inlet flow velocity,[11] and (3) equivalent ratio.[6,12] Considering the great potential to cause damages to the engine systems, nonlinear dynamics analysis of a thermoacoustic combustor with a subcritical Hopf bifurcation are needed. This partially motivated the present work.

In practice, predicting the stability behaviors of a thermoacoustic system in the deterministic aspect is not enough. A number of experimental tests[13] reveal that self-sustained thermoacoustic oscillations involve random features. For example, the amplitude and phase of limit cycle oscillations are varying from cycle to cycle.[9] And the parameters defining the combustor stability boundaries are changing from one test to another test.[13] Although the deterministic system can also manifest itself in a form of "random" motion, if the strange attractor "chaos" occurs. Culick et al.[14] applied the fraction dimension to examine the possibility of the chaotic behavior in the thermoacoustic system and denied this explanation. Therefore, the thermoacoustic system with stochastic driving/forcing will be more appropriate to characterize its response. Actually, research interests in combustion noises were initially raised in solid propellant rockets and ramjet engines.[15] Poinsot et al.[16] conducted an experimental study of a dump combustor in 1990s. They confirmed the presence of stochastic noises in the combustor by spatial maps of coherence function. By taking the effect of turbulent flow into account, Culick et al.[14] performed an excellent stochastic modelling study, when stochastic noises and combustion instability were coupled. Lieuwen[17] studied the statistical characteristics of pressure oscillations in a premixed combustor. A good prediction in probability density function (PDF) of the amplitude of the oscillations was obtained. Lieuwen and Banaszuk[18] then studied the effects of the background noises on the combustion stability from the linear aspect. The random features of the combustors were explained by considering external noise perturbations, such as cyclic variability and noise-induced transition. Noise-induced transition and stochastic bifurcations are two important and interesting noise-induced phenomena. As for the noise-induced transition, it was found that additive stochastic perturbations/disturbances could trigger the linear stable system to jump into large amplitude oscillations.[19] In addition, Waugh et al.[20] theoretically showed that pink noise (higher amplitude at lower frequency) was more effective in causing triggering in comparison with white or blue noises.

Stochastic bifurcation is mainly used to characterize the instability in a stochastic dynamic system. And there are mainly two different criterions. One is related with stochastic D-bifurcation. The other is with stochastic P-bifurcation. Stochastic D-bifurcation is characterized by the sign change of the maximum Lyapunov exponent, while stochastic P-bifurcation is characterized by a qualitative change in the probability distribution of the system response. Gopalakrishnan et al.[21] observed the stochastic P-bifurcation in a prototypical thermoacoustic system driven by an external white noise. They[22] also studied the effect of the external noise on the hysteresis region in a subcritical thermoacoustic system. It was found that increased

noise can lead to a decrease in the hysteresis region. Steinert[23] experimentally investigated the effects of external noises on a combustor's response. Both the transition process of stochastic P-bifurcation and noise-induced coherence resonance were experimentally observed. In summary, these previous works did not consider other types of noises, such as pressure-, velocity-, or combustion-related noises. The effect of combined or superimposed types of background noises resulting from acoustic, flow, and random combustion disturbances on the stochastic bifurcation and the hysteresis region is not studied. Lack of such investigations partially motivated the present work.

In this work, a noisy nonlinear model of open-ended standing-wave thermoacoustic system is proposed to study its stochastic behaviors. This is described in Sec. II. Coupling the unsteady heat release with Galerkin series expansion of the acoustic disturbances[24] provides a platform to extract time series information of the nonlinear thermoacoustic oscillations. Following the previous studies,[6,11,17,21] the limit cycle oscillations in the thermoacoustic combustors can be processed by a weakly nonlinear theory. Three different types of background noises are then introduced to the system to examine its nonlinear dynamic response. In the absence of these noises, the one dimensional (1D) open-ended thermoacoustic system we modeled is found to be associated with subcritical behaviors. By using stochastic averaging,[25] the stochastic system response is approximated into a joint Markov process. And the Fokker–Planck–Kolmogorov (FPK) equation is obtained, which governs the transition amplitude density function of the Markov process. The effect of the noise intensity on the stochastic P-bifurcation of the modelled thermoacoustic system[26] and hysteresis are systematically studied. The results are discussed in Sec. III. The key findings are summarized in Sec. IV.

II. THE NONLINEAR THERMOACOUSTIC MODEL

In the present work, a 1D Rijke-type thermoacoustic system with a flame confined inside[27] is considered, as shown in Fig. 1. L denotes the length of the tube and $\tilde{x}_f$ is the location of the heat source, i.e., the flame from the upstream open end. The flame is assumed to be acoustically compact. And both combustor ends are assumed to be acoustically open. It has been shown[28] that the dimensionless heat-driven acoustics equation along the axial direction is given as

$$\frac{\partial^2 p'}{\partial t^2} - \frac{\partial^2 p'}{\partial x^2} = (\gamma - 1)K \frac{\partial Q'}{\partial t} \delta(x - x_f), \qquad (1)$$

where p' and Q' denote the acoustic pressure and the unsteady heat release. K denotes the normalized heat power, γ is the ratio of specific heat, and $\delta(\cdot)$ is the Dirac delta function. x_f denotes the nondimensional axial location of the heat source from the upstream open end, which is normalized by the total length L. Here it is assumed that the unsteady pressure oscillation is dominated by a single mode. This assumption is widely applied in previous experimental and theoretical investigations,[23,24,29] especially on simplifed combustors such as Rijke tube. Note that this assumption is inappropriate for studying other complicated geometric propulsion systems, such as
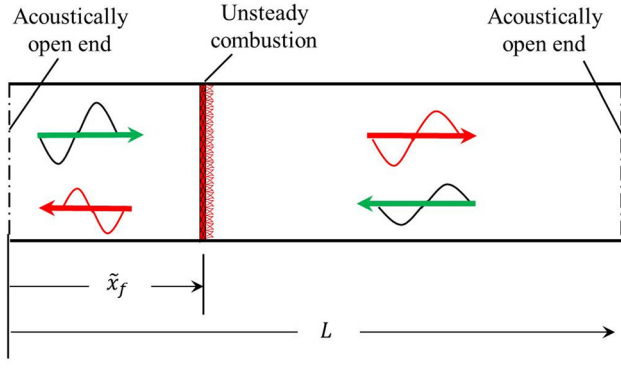
FIG. 1. (Color online) Schematic of a modelled standing-wave thermo-acoustic system with both ends acoustically open and an acoustically compact heat source confined.

rocket motors, ramjets, and augmentors, where multiple modes oscillations are present simultaneously. The pressure fluctuation is expanded as $p'(x,t) = \varphi(kx)\eta(t)$. Here $\eta(t)$ denotes the time-dependent variable. $\varphi(kx)$ is k_{th} acoustic mode function. The specific form of $\varphi(kx)$ is determined by the boundary conditions. Substituting the Galerkin expansion of p' into Eq. (1) and applying the orthogonality of the basis functions lead to

$$\ddot{\eta} + k^2\eta = 2K(\gamma-1)\dot{Q}'_f\,\varphi(kx_f), \qquad (2)$$

where the overdot denotes time derivative.

Generally, the damping effect needs to be considered, due to the heat conduction and viscosity in the boundary layer and sound radiation across the boundary open ends.[30,31] Previous studies[19,32] have confirmed that the damping effect played a significant role in determining the amplitude of thermoacoustic oscillations. Thus the present model considers the damping effect by including a damping/loss term. This enables Eq. (2) being rewritten as

$$\ddot{\eta} + k^2\eta = 2K(\gamma-1)\dot{Q}'_f\,\varphi(kx_f) - 2\xi k\dot{\eta}, \qquad (3)$$

where ξ denotes the overall damping coefficient. Here it is assumed that the term on the right hand side of Eq. (3) is "small" (the extent of "small" is given in Refs. 14 and 18). This may be due to two reasons. First, only a little amount of unsteady heat release is used to generate acoustic waves and the damping effect is limited. Second, a number of experimental and theoretical studies[33,34] show that the limit cycles can be described by a weakly nonlinear theory. Such theory is also applicable on studying Rijke-type thermo-acoustic combustor.[35] Therefore, a small factor ϵ is introduced to Eq. (3), as given as

$$\ddot{\eta} + k^2\eta = 2\epsilon K(\gamma-1)\dot{Q}'_f\,\varphi(kx_f) - 2\epsilon\xi k\dot{\eta}. \qquad (4)$$

In thermoacoustic combustors, random noise n_3(t) due to entropy fluctuations[36,37] unsteady combustion such as combustion-driven oscillations[38–40] or is present. Thus the noisy thermoacoustic model is described by

$$\ddot{\eta} + k^2\eta = 2\epsilon K(\gamma-1)\dot{Q}'_f\,\varphi(kx_f) - 2\epsilon\xi k\dot{\eta} + n_3(t). \qquad (5)$$

There may be other types of background noises, such as pressure- and velocity-coupled disturbances. To make our analysis more generalized, the noisy model can be further improved by including all three types of background noises as

$$\ddot{\eta} + k^2\eta = 2\epsilon K(\gamma-1)\dot{Q}'_f\,\varphi(kx_f) - 2\epsilon\xi k\dot{\eta} + n_3(t)$$
$$- n_1(t)\eta - n_2(t)\dot{\eta}, \qquad (6)$$

where $-n_1(t)\eta$ and $-n_2(t)\dot{\eta}$ denote the pressure- and velocity-related noise.

Following the previous work[41] in which a third-order polynomial model is used to characterize the unsteady heating release rate Q', a higher-order polynomial is proposed in this work shown as

$$Q' = b_1 p' + b_2 p'^3 + b_3 p'^5, \qquad (7)$$

where the coefficients b_1, b_2, and b_3 are constant. It is worth noting that unsteady heat release Q' predicted by using Eq. (7) is in good agreement with the experimental measurements.[41,42] Thus it is used in the following discussion.[21] Substituting Eq. (7) into Eq. (6), and taking the effect of stochastic perturbations, i.e., $n_1(t)$, $n_2(t)$, and $n_3(t)$ (Ref. 14) into account leads to

$$\ddot{\eta} + \epsilon\dot{\eta}(\alpha_1 + \alpha_2\eta^2 + \alpha_3\eta^4) + k^2\eta + n_1(t)\eta + n_2(t)\dot{\eta}$$
$$= n_3(t), \qquad (8)$$

where $\alpha_1 = 2\xi k - 2b_1 K(\gamma-1)\varphi^2(kx_f)$, $\alpha_2 = -6b_2 K(\gamma-1)\varphi^4(kx_f)$, and $\alpha_3 = -10b_3 K(\gamma-1)\varphi^6(kx_f)$. $n_1(t)$, $n_2(t)$, and $n_3(t)$ describe the stochastic perturbations. $n_1(t)$ denotes pressure-coupled noisy excitation. It is acoustics-related. $n_2(t)$ is stochastic velocity-coupled noisy perturbation and it is flow (vorticity)-coupled. $n_3(t)$ denotes an external stochastic forcing, which can characterize random disturbances from unsteady combustion. The stochastic sources $n_1(t)$, $n_2(t)$, and $n_3(t)$ are assumed to be independent of the amplitude of $\eta(t)$. The three noisy terms are assumed to be uncorrelated. Furthermore, they are assumed to involve the stochastic properties as follows:

$$\langle n_1(t)\rangle = 0, \ \langle n_2(t)\rangle = 0, \ \langle n_3(t)\rangle = 0,$$
$$\langle n_1(t)n_1(t+\tau)\rangle = D_1\delta(\tau),$$
$$\langle n_2(t)n_2(t+\tau)\rangle = D_2\delta(\tau),$$
$$\langle n_3(t)n_3(t+\tau)\rangle = D_3\delta(\tau)$$
$$\langle n_1(t)n_2(t+\tau)\rangle = \delta(\tau), \qquad (9)$$

$\langle\cdot\rangle$ is the expectation operator and D_1, D_2, D_3 are the noise's intensity. Clearly the noise $n_1(t)$ and $n_2(t)$ are multiplicative and the external combustion noise $n_3(t)$ is additive.

By applying stochastic averaging[43] to approximate the nonlinear stochastic response, a pair of a slowly varying process is needed. A suitable transformation is implemented as

$$\eta(t) = A(t)\cos\theta, \ \dot{\eta}(t) = -kA(t)\sin\theta, \ \theta = kt + \phi(t), \qquad (10)$$

where $A(t)$ denotes the amplitude of the system response and $\phi(t)$ is the phase. Then Eq. (8) can be rewritten into the following pair of ODE (ordinary differential equation) equations in term of A and ϕ as

$$\dot{A} = -\epsilon A \, \sin^2\theta \big(\alpha_1 + \alpha_2 A^2 \cos^2\theta + \alpha_3 A^4 \cos^4\theta\big)$$
$$+ \frac{A \sin\theta \cos\theta}{k} n_1(t) - A \sin^2\theta \, n_2(t) - \frac{\sin\theta}{k} n_3(t),$$

$$\text{(11)}$$

$$\dot{\phi} = -\epsilon \sin\theta \cos\theta \big(\alpha_1 + \alpha_2 A^2 \cos^2\theta + \alpha_3 A^4 \cos^4\theta\big)$$
$$+ \frac{\cos^2\theta}{k} n_1(t) - \sin\theta \cos\theta \, n_2(t) - \frac{\cos\theta}{Ak} n_3(t). \quad \text{(12)}$$

Due to the assumption that ϵ is small, (A, ϕ) can be approximated as a joint Markov process.[44–46] By using stochastic averaging, the corresponding Itô equation can be obtained as[47]

$$dA = \left(-\frac{\epsilon\alpha_3 A^5}{16} - \frac{\epsilon\alpha_2 A^3}{8} - \frac{\epsilon\alpha_1 A}{2} + \frac{5k^2 D_2 + 3D_1}{16k^2} A + \frac{D_3}{4k^2 A} \right) dt$$
$$+ \sqrt{\frac{A^2 D_1 + 3A^2 k^2 D_2 + 4D_3}{8k^2}} \, dW_1, \quad \text{(13)}$$

$$d\phi = \sqrt{\frac{3A^2 D_1 + A^2 k^2 D_2 + 4D_3}{8k^2 A^2}} \, dW_2, \quad \text{(14)}$$

where dW_1 and dW_2 denote two independent Wiener processes (Brownian motion).[48]

It is worth noting that the amplitude $A(t)$ does not depend on ϕ as shown in Eq. (13), so it will be convenient to develop a 1D probability density for A, rather than a joint density for A and ϕ. The transition density function $P(A, t)$ of the 1D Markov process A is governed[49] by the following Fokker–Planck–Kolmogorov (FPK) equation as

$$\frac{\partial P(A,t)}{\partial t} = \frac{\partial}{\partial A}\left\{ \left(\frac{\epsilon\alpha_3 A^5}{16} + \frac{\epsilon\alpha_2 A^3}{8} + \frac{\epsilon\alpha_1 A}{2} \right. \right.$$
$$\left. - \frac{5k^2 D_2 + 3D_1}{16k^2} A - \frac{D_3}{4k^2 A} \right) P(A,t) \Big\}$$
$$+ \frac{\partial^2}{\partial A^2}\left\{ \left(\frac{A^2 D_1 + 3A^2 k^2 D_2 + 4D_3}{16k^2} \right) P(A,t) \right\}.$$

$$\text{(15)}$$

Then the drift coefficient $m(A)$ and the diffusion coefficient $b(A)$ can be obtained as

$$m(A) = -\frac{\epsilon\alpha_3 A^5}{16} - \frac{\epsilon\alpha_2 A^3}{8} - \frac{\epsilon\alpha_1 A}{2}$$
$$+ \frac{5k^2 D_2 + 3D_1}{16k^2} A + \frac{D_3}{4k^2 A},$$

$$b(A) = \frac{A^2 D_1 + 3A^2 k^2 D_2 + 4D_3}{8k^2}. \quad \text{(16)}$$

The stationary probability density function can be obtained by setting $\partial P(A,t)/\partial t = 0$, as shown as

$$P(A) = \mathcal{N} \exp\left(\int \frac{2m(A) - b'(A)}{b(A)} dA \right), \quad \text{(17)}$$

where $\mathcal{N}$ is a normalization constant so that $\int_0^\infty P(A)dA = 1$. In addition, the peaks of the distribution $P(A)$ is determined by finding the roots of the equation below:

$$f(A_e) = \epsilon\alpha_3 A_e^5 + 2\epsilon\alpha_2 A_e^3 + \left(8\epsilon\alpha_1 + D_2 - \frac{D_1}{k^2} \right) A_e$$
$$- \frac{4D_3}{A_e k^2} = 0, \quad \text{(18)}$$

where A_e is the amplitude corresponding to the extreme of the amplitude density distribution.

III. RESULTS AND DISCUSSION

The stochastic behaviors of the modelled open-ended standing-wave thermoacoustic system in the presence of three types of background noises are discussed and summarized. Before we discuss the noise effect, the nonlinear behaviors of the deterministic thermoacoustic system are studied, i.e., $D_1 = 0$, $D_2 = 0$, $D_3 = 0$. Figure 2 shows the bifurcation diagram with respect to the oscillations amplitude A and the heating power K. In the absence of stochasticity, the distinguished hysteresis zone (denoted by the shaded cyan) is clearly observed. It indicates that the thermoacoustic system we studied is subcritical. Furthermore, an Andronov–Hopf bifurcation point is identified and denoted by P_1 and a fold bifurcation point is denoted by P_2. When the heating power K is less than 2.94 (or larger than 3.12), the system is globally stable (unstable). Otherwise, a stable steady state and a stable limit cycle coexist. In the following studies, the heating power K is chosen to be the only variable to define the operation condition of the thermoacoustic system.

A. Effect of each type of background noises

The background noise effect can be studied in different combinations. However, it would be reasonable to study the effect of each type of background noise on the hysteresis and stochastic behaviors of the system first. The combination of each of the two types of background noises will be discussed in Sec. III B. Figure 3 shows the effect of the pressure-coupled noise n_1 on the hysteresis region and the stochastic transition, as $D_2 = 0$ and $D_3 = 0$.

It is obtained by evaluating the dependence of the roots number of Eq. (16) on the heating power K and the noise intensity D_1 we consider. Curve l_1 and l_2 denote the critical boundary about the presence of the peak of $P(A)$ with different amplitudes. The rectangular cyan shaded region denotes the hysteresis region with bi-stable status in the absence of these noises, i.e., $D_1 = 0$, $D_2 = 0$, $D_3 = 0$. The pink shaded region denotes the hysteresis region with bimodal stationary probability density with $D_1 \neq 0$. It is obvious that the pink shaded hysteresis region for $D_1 \neq 0$ and the cyan shaded hysteresis for $D_1 = 0$ are not overlapped as shown in Fig. 3(a). With the increase of the pressure-coupled noise intensity D_1, the width of the hysteresis region is decreased. In addition, the pink shaded region is shifted to a decreased heating power K. Thus the stable region is decreased too.

Three points, i.e., P_1, P_2, P_3 in the bifurcation diagram as shown in Fig. 3(a) are selected to evaluate the corresponding stationary probability distributions (PDFs) at three representative regions. Here the same thermoacoustic system is chosen by setting $K = 2.8$ and the intensity of the pressure-coupled
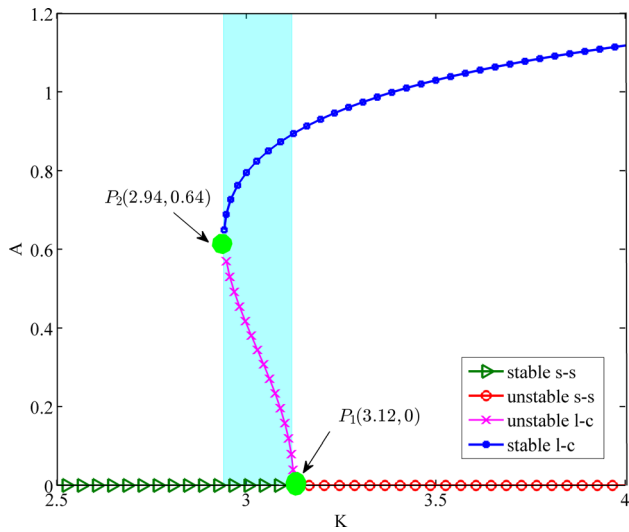
J. Acoust. Soc. Am. **143** (1), January 2018

Li *et al.*   63

FIG. 2. (Color online) Calculated bifurcation diagram of the modelled deterministic thermoacoustic system in the phase plane of the heating power K and the oscillation amplitude A. s-s: steady state, l-c: limit cycle, as $\gamma = 1.4$, $\bar{u} = 0.5$ m/s, $\bar{p} = 1$ atm, $x_f = 0.25$, $\xi = 0.1$.

noise (acoustics-related) to three different values. The corresponding PDFs for the amplitude A are given in Fig. 3(b). The analytical solutions in Fig. 3(b) are denoted by the brown lines and obtained directly by discretizing Eq. (17). The dotted lines are obtained by Monte Carlo simulations. The number of integral path is 500 and each path is obtained[50,51] by integrating Eq. (8). It can be seen from Fig. 3(b) that the brown solid lines agree well with the dotted lines. These excellent agreements confirm that the approximated analytical prediction is applicable to study the stochastic behaviors of the thermoacoustic

system in the presence of pressure-coupled noises we are interested in. Such an approach is applied to analyze the following cases to validate the analytical prediction for other types of background noises.

When the pressure-coupled noise n_1 is small (e.g., P_1), it can be seen from Fig. 3(b) that the blue-circled line has a Dirac function like distribution. The stationary amplitude distribution $P(A)$ is more close to zero, if the intensity of D_1 is constrained in the lower triangular region of Fig. 3(a). That is to say, the thermoacoustic system will arrive at a steady state, if the pressure-coupled perturbation is small. However, if the intensity of the pressure-coupled perturbations is increased further so that D_1 is within the shaded pink region of Fig. 3(a), the Dirac function like $P(A)$ is turn to be like a crater, which is denoted by the green triangular dotted curve (P_2). In this case, the probability density $P(A)$ has a minimum and a maximum peak, and such craterlike PDF has been experimentally observed in Ref. 52. Further increasing the noise intensity D_1 to the upper trapezoid regions results in a Gaussian-type distribution $P(A)$ for a larger amplitude, which can be seen by the red square dots (P_3) as shown in Fig. 3(b). Under this condition, large amplitude thermoacoustic oscillations are triggered by large-amplitude pressure-coupled perturbations, when the thermoacoustic system is at the global stable region. Therefore, the pressure-coupled perturbations change the combustor's dynamic behavior in a qualitative way: large-amplitude pressure-coupled noise can destabilize the linear stable system qualitatively, even when the thermoacoustic system is far away from the critical bifurcation points. In addition, two different transition processes are identified and stochastic P-bifurcation is observed. One is from a Dirac function-like
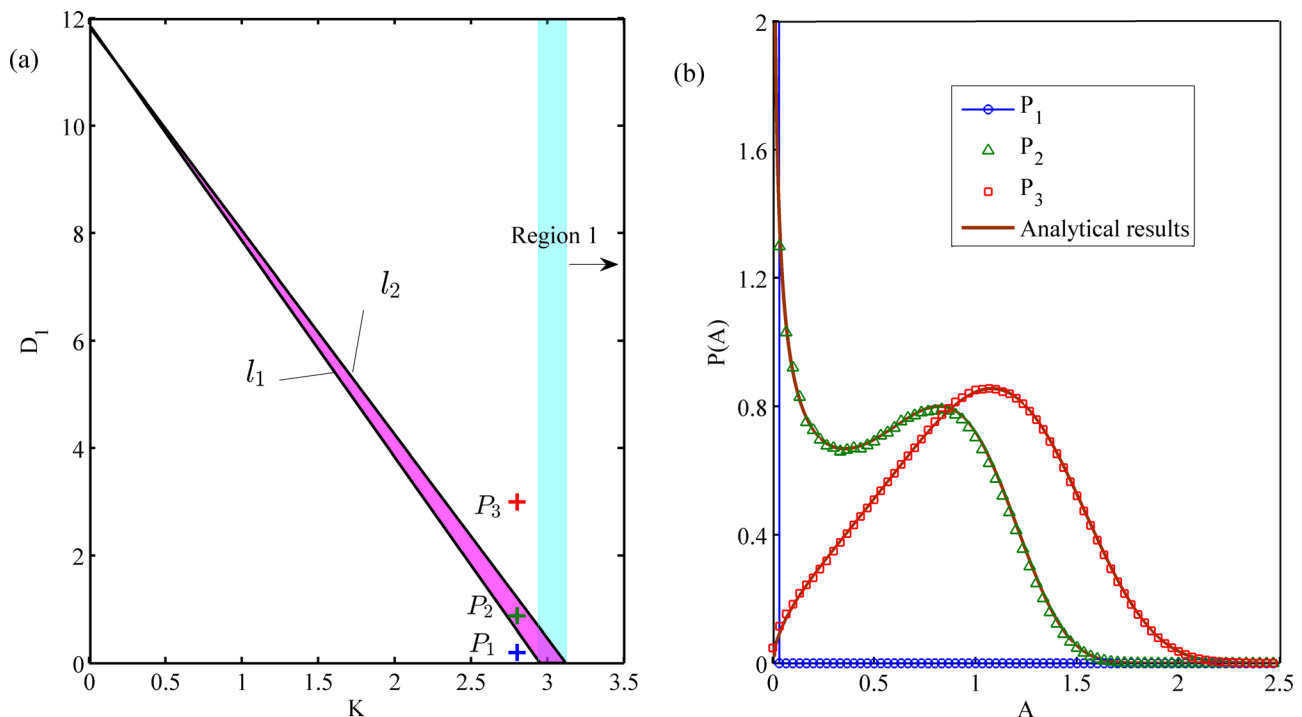

FIG. 3. (Color online) (a) Calculated stochastic bifurcation diagram in the phase plane of (K, D_1) for the simplified 1D Rijke-type thermoacoustic system; (b) variation of the probability density distribution $P(A)$ with the oscillation amplitude A at different noise intensities D_1, as $b_1 = 1$, $b_2 = 1.2$, $b_3 = -3$, $k = \pi$, $x_f = 1/4$, $D_2 = 0$, $D_3 = 0$; P_1 (2.80, 0.20), P_2 (2.80, 0.88), P_3 (2.8, 3).
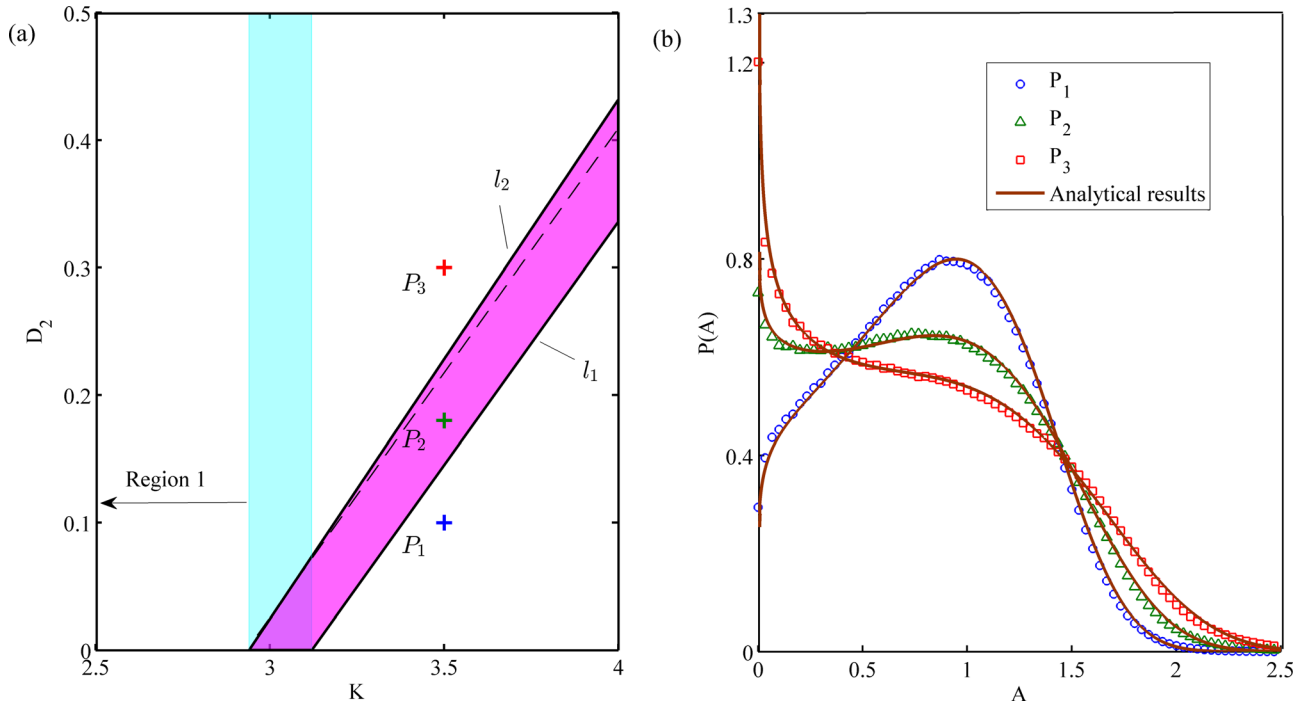
FIG. 4. (Color online) (a) Calculated stochastic bifurcation diagram in the phase plane of (K, D_2) for the simplified 1D Rijke-type thermoacoustic system; (b) variation of stationary probability density distribution $P(A)$ with the amplitude A at different damping noise intensity D_2, as $b_1 = 1$, $b_2 = 1.2$, $b_3 = -3$, $k = \pi$, $x_f = 1/4$, $D_1 = 0$, $D_3 = 0$. P_1 (3.5, 0.10), P_2 (3.5, 0.18), P_3 (3.5, 0.3).

distribution to a craterlike distribution. The other is from the craterlike distribution to a Gaussian-type distribution. Considering that both transitions are associated with craterlike PDF, we define it as the first type of stochastic P-bifurcation.

Figure 4 illustrates the effect of the velocity-coupled noise n_2 on the modelled standing-wave thermoacoustic system, as $D_1 = 0$ and $D_3 = 0$. The calculated stochastic bifurcation diagram in the phase plane of (K, D_2) is shown in Fig. 4(a). Now the pink shaded region denotes the hysteresis for the stochastic system, as $D_1 = 0$, $D_2 \neq 0$, $D_3 = 0$. Different from the effect of the pressure-coupled noise n_1 as shown in Fig. 3(a), increased velocity-coupled noise n_2 cannot only increase the width of the pink shaded hysteresis region, but also shift the hysteresis region to the linearly unstable region. This is clearly shown in Fig. 4(a).

Similarly, three representative points, i.e., P_1, P_2, P_3 are selected, as $K = 3.5$. Under this operating condition, the thermoacoustic system is globally unstable from the deterministic aspect. Their corresponding PDFs for the amplitude A are shown in Fig. 4(b). When the velocity-coupled noise n_2 is small, the blue circle dotted line P_1 exhibits a Gaussian-type probability density distribution with a large amplitude, which means that the small-amplitude velocity-coupled noise n_2 does not affect the system response significantly. When the amplitude of n_2 is increased to be in the shaded region as shown in Fig. 4(a), a craterlike PDF is clearly observed. Further increasing the amplitude of the velocity-coupled noise n_2 (e.g., P_3) leads to small-amplitude oscillations, which can be seen by the red square dotted line. In this case, the stabilizing effect of the velocity-coupled noise $n_{2(t)}$ becomes obvious and large-amplitude oscillations are

suppressed to be small-amplitude perturbations. In addition, although $P(A)$ is maximized at zero, but it scatters more widely than the Dirac-like distribution as shown in Fig. 3(b). Therefore, the thermoacoustic system will not be in a steady state, but oscillates with a small amplitude. Finally, the first type stochastic P-bifurcation as we define before is observed, as the noise intensity D_2 is increased.

Figure 5 shows the effect of the additive combustion-related noise n_3 on the Rijke-type thermoacoustic system, as $D_1 = 0$ and $D_2 = 0$. The calculated stochastic bifurcation diagram in the phase plane of (K, D_3) is illustrated in Fig. 5(a). It can be seen that increasing the intensity of n_3 leads to the width of the pink shaded hysteresis region being decreased, and shifts the pink shaded region to the linear stable region, so that the stable region is decreased. Such analytical prediction shows a qualitatively good agreement with the experimental measurements.[21,22] Although the external combustion-related noise n_3 exerts similar effects on the hysteresis width and stable region with pressure-coupled noise D_1, its destabilizing effect is much limited than that of the pressure-coupled noise D_1, which can be seen from the small tilt and the existence of the absolute stable *Region 1* in Fig. 5(a). It is worth noting that the external combustion noise n_3 does not affect combustor's dynamic behaviors, when the thermoacoustic system is operated in *Region 1*.

Figure 5(b) shows the calculated PDF at three representative points (denoted by P_1, P_2, P_3), when the thermoacoustic system is linearly stable, e.g., $K = 2.923$. The PDFs with smaller peaks are depicted in the inner embedded figure for better description. When the thermoacoustic system is perturbed by small-amplitude noises (see point P_1), a Rayleigh type distribution is observed. $P(A)$ has only one local
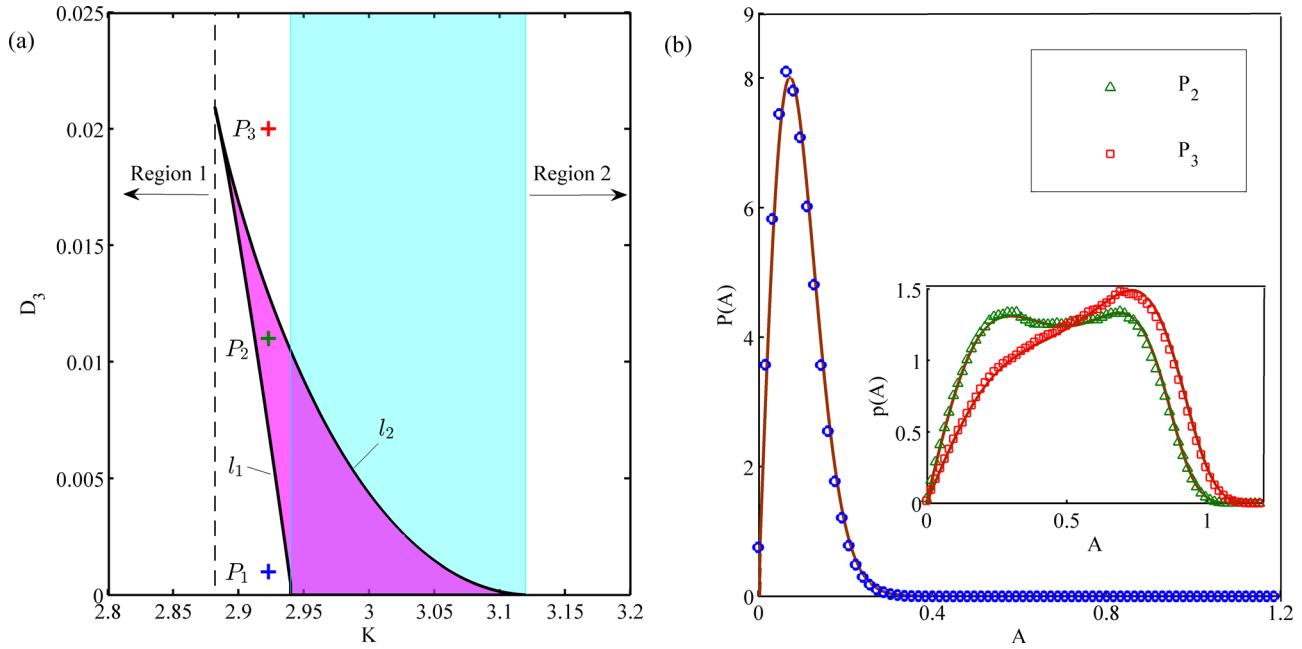
FIG. 5. (Color online) (a) Stochastic bifurcation diagram in the phase plane of (K, D_3) for the simplified 1D Rijke-type thermoacoustic system; (b) Stationary probability density distribution $P(A)$ varied with the amplitude A at different external combustion-related noise intensities D_3, as $b_1 = 1$, $b_2 = 1.2$, $b_3 = -3$, $k = \pi$, $x_f = 1/4$, $D_1 = 0$, $D_2 = 0$. P_1 (2.923, 0.001), P_2 (2.923, 0.011), P_3 (2.923, 0.02).

maximum in the vicinity of zero. When the noise intensity D_3 is increased further (see point P_2), a new type of PDF with two maximum peaks and one valley is obtained. Such shape of PDF has already been observed in the experimental measurements.[11,23] Further increasing the noise intensity (see point P_3) leads to the thermoacoustic system being "locked" in a large-amplitude limit cycle, and the peak at the local small amplitude disappears. Now the amplitude distribution becomes unimodal again. Thus two different transition processes are observed. One is from a Rayleigh-type distribution for a smaller amplitude to bimodal distribution with double maximum peaks. The other is from the bimodal distribution with double peaks to unimodal distribution for a larger amplitude. Clearly, the stochastic P-bifurcation induced by the external combustion noise n_3 is different from that in the previous two cases (pressure- or velocity-coupled noises). As for the transitions related to PDF with two maximum peaks and one trough, we define it as the second type of stochastic P-bifurcation in the present work. It is worth noting that when the system undergoes periodic oscillations with double stable peaks, it corresponds to the bi-stable condition with a steady state and a stable limit cycle oscillations in the deterministic system. Therefore, introducing the combustion-related noise such as $n_3(t)$ does not change the system's dynamic in qualitative ways, but exert quantitative effects on the combustion responses.

B. Effect of two combined background noises

Figure 6 illustrates the statistical features of the thermoacoustic system by introducing both the pressure-coupled noise $n_1(t)$ and the velocity-coupled noise $n_2(t)$ simultaneously, as the additive external combustion noise is set to $D_3 = 0$. The calculated 3D stochastic bifurcation diagram with respect the heating power K and the noise intensity D_1 and D_2 Fig. 6(a).

The green plane is for $K = 2.94$ and the yellow is for $K = 3.12$. These two vertical planes are the boundaries of the hysteresis and the space between them is the hysteresis region with bi-stable status for a deterministic case. The boundaries of the hysteresis region with the bimodal PDF for the stochastic system are denoted by the tilt planes in blue and red, between which the space is a hysteresis region with the bimodal PDF. Due to the effect of the combined noises, the hysteresis region with the bimodal distribution as shown in Fig. 6(a) is shifted into both the global stable region and the global unstable region. Therefore, a proper combination of D_1 and D_2 can either stabilize the linearly unstable thermoacoustic system, or destabilize the linearly stable thermoacoustic system. The two possibilities are mainly determined by the specific combination of the pressure-coupled noise n_1 and the velocity-coupled noise n_2. Figure 6(b) shows that there are mainly three regions in the plane of (D_1, D_2): the upper colorless *Region 1*, the lower colorless *Region 2* and the middle colored region. The pink shaded region denotes the hysteresis with bimodal distribution when $K = 2.94$, and the cyan shaded region is the hysteresis for $K = 3.12$. When the pressure-coupled noise and the velocity-coupled noise are configured within *Region 1* (*Region 2*), the destabilizing (stabilizing) effect plays a dominant role.

Four representative points are selected in four different regions, and their corresponding PDFs are illustrated in Figs. 6(c) and 6(d). As the noise intensity is increased, it can be seen that the first type of stochastic P-bifurcation occurs in Figs. 6(c) and 6(d). In addition, there is a large similarity in the calculated PDFs, no matter whether the thermoacoustic system is in the global stable region [Fig. 6(c)] or in the global unstable region [Fig. 6(d)].

Figure 7 summarizes the statistical features of the modelled Rijke-type thermoacoustic system, when it is perturbed
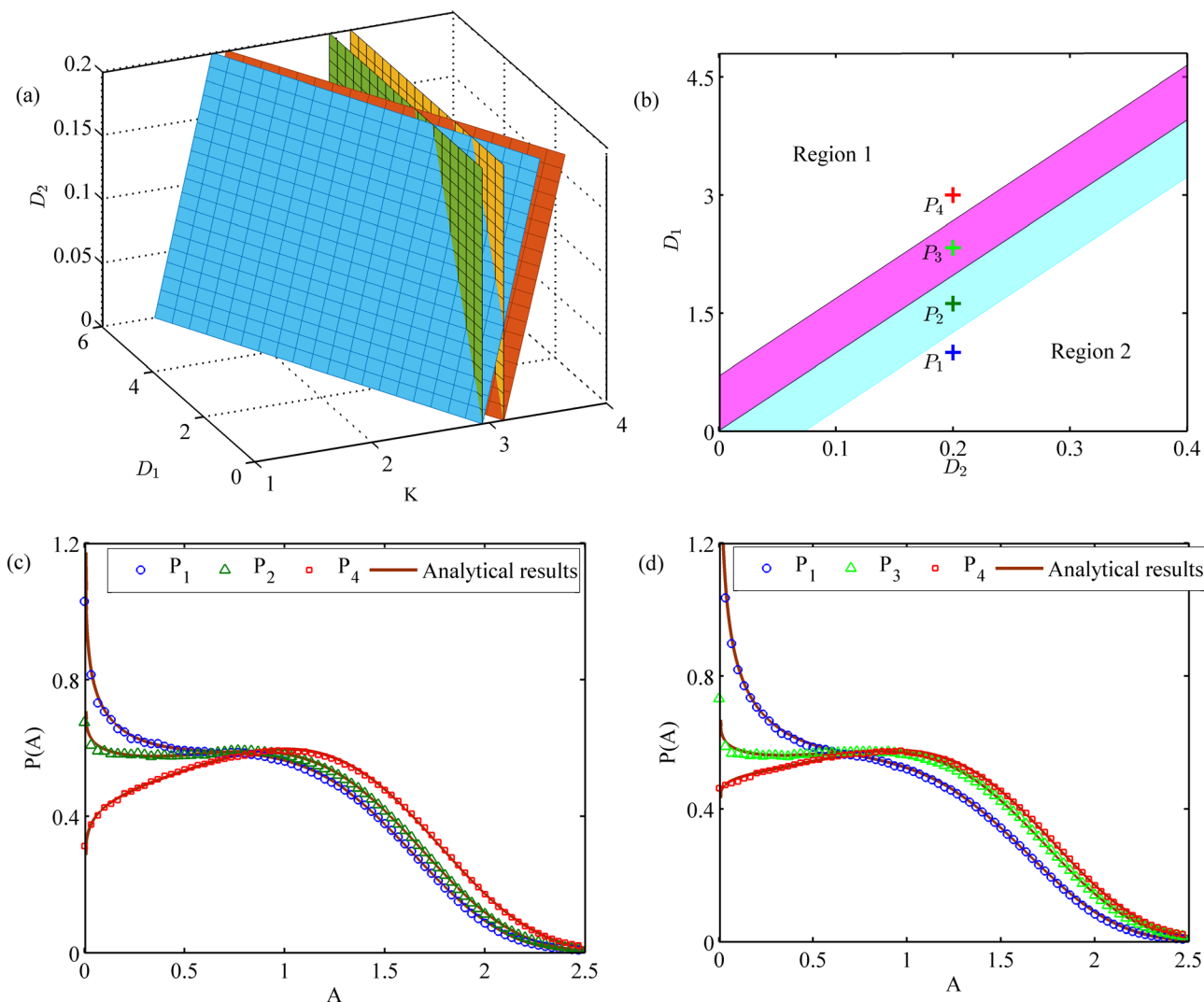
FIG. 6. (Color online) Stochastic bifurcation diagram in the phase plane of (K, D_1, D_2) for the simplified 1D Rijke-type thermoacoustic system, as $D_3 = 0$; (b) The top-down view of (a); The pink (cyan) shaded part is the deterministic boundary enclosed by the bimodal region when $K = 2.94$ ($K = 3.12$). $P_1(0.2, 1.0)$, $P_2(0.2, 1.62)$, $P_3(0.2, 2.33)$, $P_4(0.2, 3)$; (c) Stationary probability density distribution $P(A)$ varied with the amplitude A at different noise intensities D_1 as $D_2 = 0$, $D_3 = 0$, $K = 3.13$; (d) Stationary probability density distribution $P(A)$ varied with the amplitude A at different noise intensities D_1 as $D_2 = 0.2$, $D_3 = 0$, $K = 2.93$.

by the pressure-coupled noise n_1 and the combustion-related noise n_3 simultaneously. Figure 7(a) shows a stochastic bifurcation diagram with respect to the heating power K and the pressure-coupled noise intensity D_1 and the external combustion noise intensity D_3. Increasing either D_1 or D_3 shifts the hysteresis region to the decreased heating power, as that the stable region is decreased. Figure 7(b) gives a top-down view of Fig. 7(a). The red shaded hysteresis region is induced by the external combustion noise, $n_3(t)$ and the blue color denotes that by the pressure-coupled noise $n_1(t)$. It is obvious that the pressure-coupled noise $n_1(t)$ plays a more important role in determining the stability boundary of the thermoacoustic system. In addition, a cyan shaded region, where the stochastic thermoacoustic system is globally stable, is observed in Fig. 7(b).

It is interesting to note that this region as shown in Fig. 7(b) is not observed in Fig. 3(a), when the system is perturbed by the pressure-coupled noise $n_1(t)$. Therefore, the occurrence of the cyan shaded region confirms the contribution of the

addition of the external noise D_3. So combining with the pressure-coupled noise $n_1(t)$ makes the role of the external combustion-related noise $n_3(t)$ more complicated.

The external noise can counteract the pressure-coupled noise's destabilizing effect, when the heating power K is small. As $D_3 = 0.001$, the stochastic bifurcation diagram with respect to the pressure-coupled noise and the heating power K is illustrated in Fig. 7(c). The shaded pink region denotes the bimodal distribution. It divides the whole region into a lower triangular colorless region and upper trapezoid colorless region. With the increase of the pressure-coupled noise intensity D_1, the hysteresis region moves to the left part. Similar trend is observed, when only the pressure-coupled noise is exerted on the thermoacoustic system. Similarly three representative points P_1, P_2, and P_3 are selected in three different regions and their corresponding PDFs are calculated and shown in Fig. 7(d). It can be seen that the second type of stochastic P-bifurcation occurs. Such type of P-bifurcation is also observed, when the thermoacoustic system is perturbed
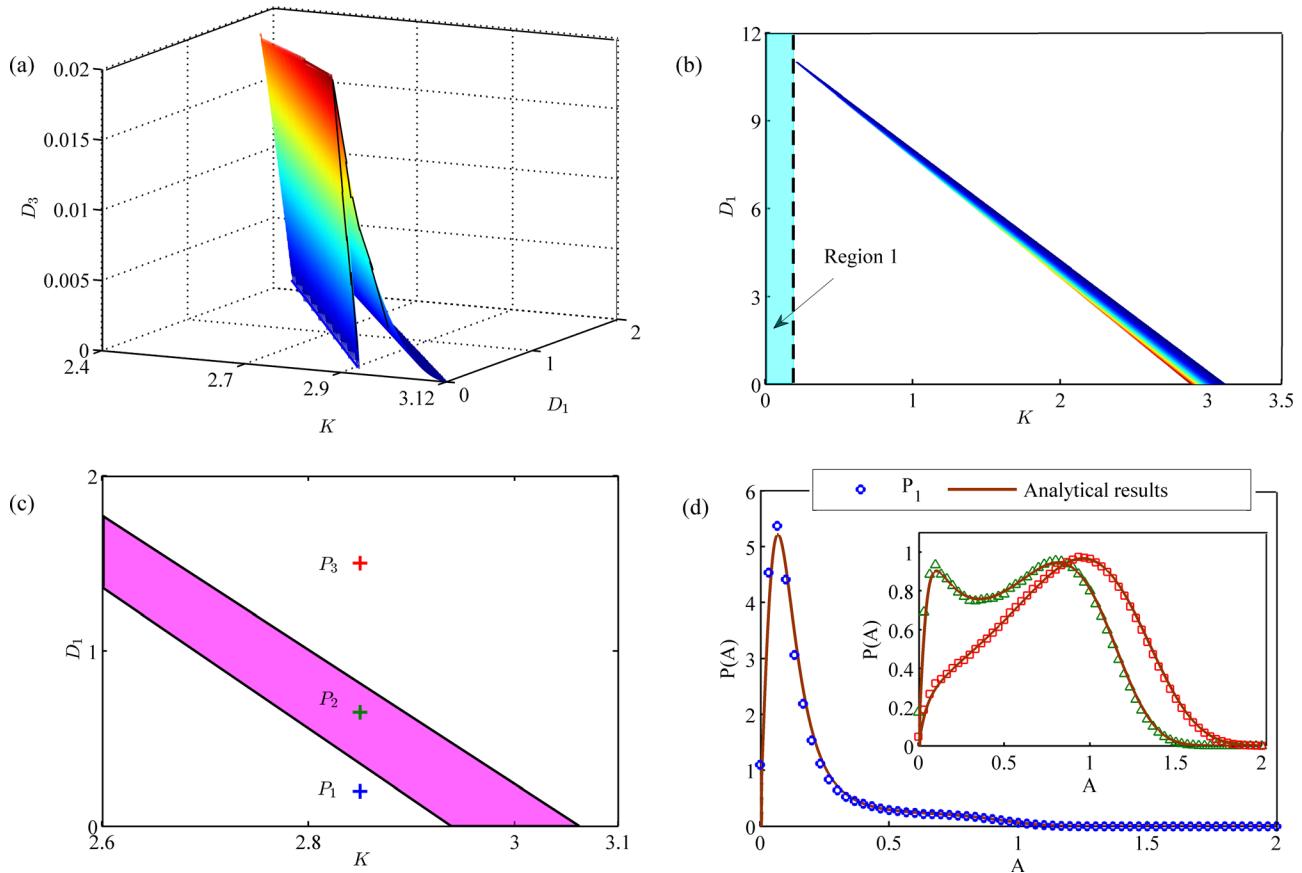
J. Acoust. Soc. Am. **143** (1), January 2018

Li *et al.*   67

FIG. 7. (Color online) (a) Stochastic bifurcation diagram in the phase plane of (K, D_1, D_3) for the simplified 1D Rijke-type thermoacoustic system, as $D_2 = 0$; (b) The top-down view of (a); (c) Stochastic bifurcation diagram in the phase of (K, D_1). $P_1 = (2.85, 0.2)$, $P_2(2.85, 0.65)$, $P_3(2.85, 1.5)$, as $D_2 = 0$, $D_3 = 0.001$; (d) Stationary probability density distribution $P(A)$ varied with the amplitude A at different noise intensities D_1, as $D_2 = 0$, $D_3 = 0.001$.

by the external combustion-related noise $n_3(t)$ only. This indicates that the external noise $n_3(t)$ plays a dominant role in determining the transition process.

Figure 8 illustrates the calculated statistical features of the thermoacoustic system, when it is perturbed by the velocity-coupled noise n_2 and the external noise n_3 simultaneously. It can be seen from Fig. 8(a) that the hysteresis region with a bimodal distribution is shifted to the increased heating power K. Figure 8(b) gives the top-down view of Fig. 8(a). The curves l_1 and l_2 denote the hysteresis boundary with respect to the heating power K and the noise intensity D_2, as $D_3 = 0$. Curve l_3 is obtained by mapping the peak of 3D graph into the phase plane (K, D_2). Compared with the external combustion-related noise $n_3(t)$, the velocity-coupled noise $n_2(t)$ plays a dominant role in determining the stability boundary of the thermoacoustic systems. It also shifts the hysteresis region towards the linearly unstable region, which expands the stable region. The addition of the external noise $n_3(t)$ counteracts the stabilizing effect of the velocity-coupled noise $n_2(t)$ to certain extent, which is illustrated by the area enclosed by l_1 and l_3. Figure 8(c) shows the stochastic diagram in the plane of (K, D_2), as the external noise intensity is set to $D_3 = 0.001$. It has been seen that the external noise does not affect the stochastic bifurcation diagram of (K, D_2) qualitatively, but quantitatively decrease the width of the hysteresis. Figure 8(d) shows the PDFs of three selected points, P_1, P_2, and P_3 as shown in Fig. 8(c). Clearly, the transition process is

found to be the second type of stochastic P-bifurcation as defined before. Such type of P-bifurcation is observed in the system when either only the external noise, or the external noise with the pressure-coupled noise is present. Therefore, the external combustion-related noise $n_3(t)$ is revealed to determine the transition process of the stochastic thermoacoustic system.

IV. DISCUSSION AND CONCLUSIONS

The present work considers the effects of three different types of background noises on the nonlinear dynamics of an open−open standing wave thermoacoustic system. These noises include (1) pressure-coupled noise, (2) velocity-coupled noise, and (3) external combustion-related stochastic noise. For this, a noisy thermoacoustic model with a premixed flame confined is developed first. A fifth-order polynomial formulation is proposed to describe the unsteady heat release rate from the flame. In the absence of these noises, the thermoacoustic system is shown to be subcritical and a hysteresis region is clearly observed. Acoustic disturbances in the modeled system are numerically expanded by using Galerkin series. The coupling between the acoustic disturbances and unsteady heat release thus provides a platform to study the nonlinear dynamics of the thermoacoustic system in time domain. The system's random response is approximated into Markov process via stochastic averaging.
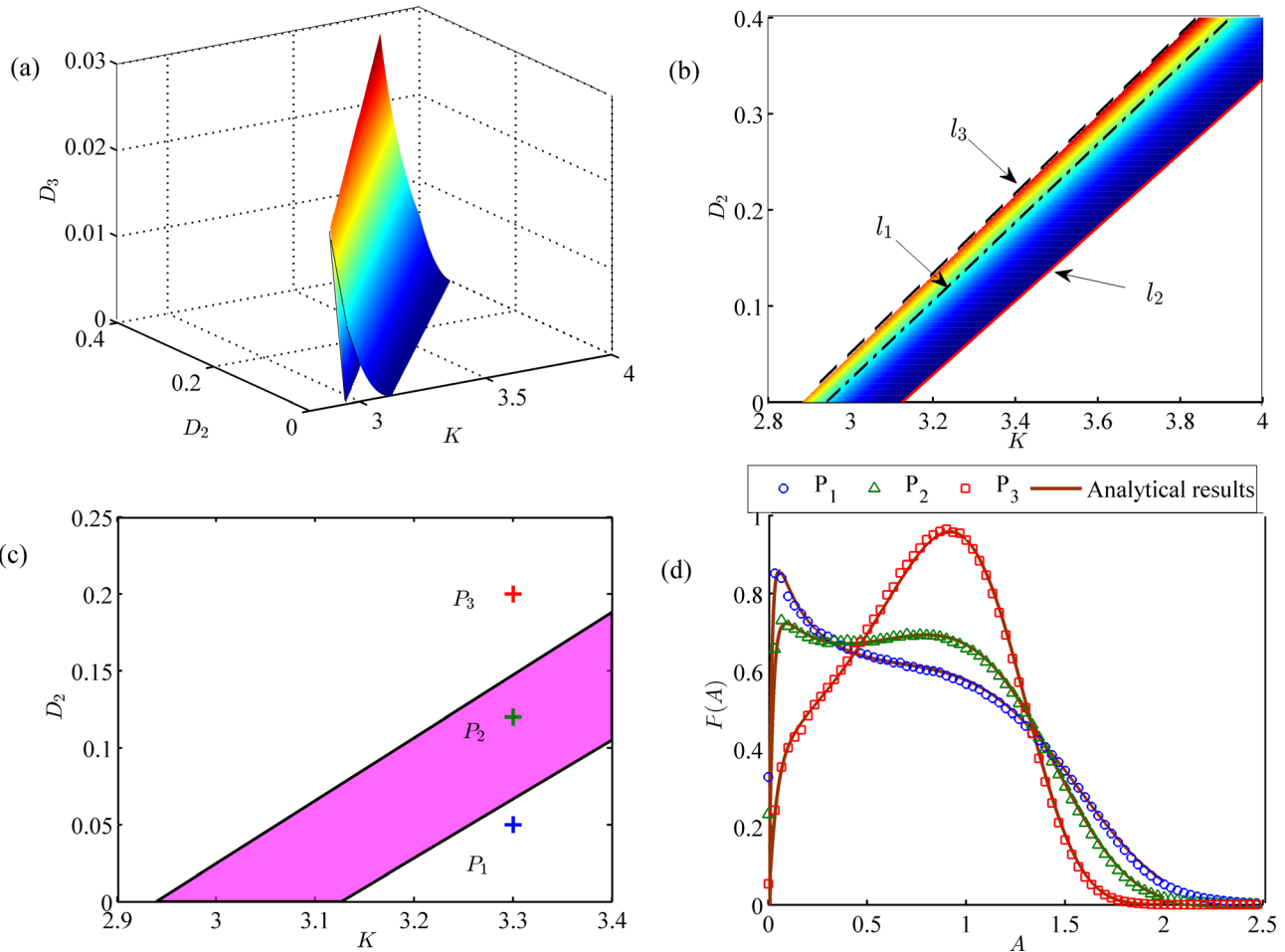
FIG. 8. (Color online) Stochastic bifurcation diagram in the phase plane of (K, D_2, D_3) for the simplified 1D Rijke-type thermoacoustic system, as $D_1 = 0$; (b) The top-down view of (a); (c) stochastic bifurcation diagram in the phase of (K, D_2). $P_1(3.3, 0.05)$, $P_2(3.3, 0.12)$, $P_3(3.3, 0.2)$, as $D_1 = 0$, $D_3 = 0.001$; (d) stationary probability density distribution $P(A)$ varied with the amplitude A at different noise intensities D_1, as $D_2 = 0$, $D_3 = 0.001$.

By solving the corresponding FPK equation, the stationary PDF is analytically obtained to determine the system's response.

The effects of three different types of background noises on the hysteresis, stable region, and transition processes are then systematically studied. For this, the thermoacoustic system is disturbed by adding these noises one type at a time. It is found that the pressure-coupled noise and velocity-coupled noise have dramatic different effects on the system's stability, but share the same transition process. However, the pressure-coupled noise and the external noise are found to have similar effects on the system's stability, but have different transition processes. Furthermore, increasing the intensity of either the pressure-coupled noise or the external combustion noise can decrease the hysteresis width and stable region. The external noise is shown to have negligible effect on decreasing the stable boundary. On the contrary, increasing the velocity-coupled noise leads to the width of the hysteresis region being increased and the stable region being expanded. As for the transition process, it is found that stochastic P-bifurcation describes the process very well. And two different types of stochastic P-bifurcations are observed and identified. The first type of stochastic P-bifurcation is characterized by a transition between a unimodal PDF and a bimodal craterlike PDF. This type of P-bifurcation is identified, when the thermoacoustic system is forced by either the pressure-coupled or the velocity-coupled noise. The second type of P-bifurcation is characterized by a transition between a unimodal PDF and a bimodal PDF with two peaks and one trough. This bifurcation is observed, when the system is disturbed by the external noise.

Finally, the effect of combined two types of background noises on the thermoacoustic system's stability is evaluated. When the thermoacoustic system is disturbed by the two multiplicative noises such as the pressure- or velocity-coupled noises simultaneously, the combined noise can either stabilize the globally unstable system, or destabilize the globally stable system. It depends strongly on the specific combination of the two types of the background noises. The transition process is found to be the first type of stochastic P-bifurcation. If the combined noises consist of a multiplicative noise and an additive noise, such as (1) the pressure-coupled noise with the external combustion noise, or (2) the velocity-coupled noise with the external combustion noise, then the multiplicative noise is found to play a dominant role in determining the stability boundary. Furthermore, the external combustion noise (chemical reaction) is shown to determine the transition processes.

J. Acoust. Soc. Am. **143** (1), January 2018

Li et al.   69

[1]H. Gotoda, H. Nikimoto, T. Miyano, and S. Tachibana, "Dynamic properties of combustion instability in a lean premixed gas-turbine combustor," Chaos **21**, 013124 (2011).

[2]S. Cho and S. Lee, "Characteristics of thermoacoustic resonance in a ducted burner," J. Acoust. Soc. Am. **105**, 3584–3587 (1999).

[3]J. W. S. B. Rayleigh, *The Theory of Sound* (Macmillan, London, UK, 1877), pp. 118–148.

[4]U. Zalluhoglu and N. Olgac, "A study of Helmholtz resonators to stabilize thermoacoustically driven pressure oscillations," J. Acoust. Soc. Am. **139**, 1962–1973 (2016).

[5]Z. Zhong and D. Zhao, "Time-domain characterization of the acoustic damping of a perforated liner with bias flow," J. Acoust. Soc. Am. **132**, 271–281 (2012).

[6]J. Moeck, M. Bothien, S. Schimek, A. Lacarelle, and C. Paschereit, "Subcritical thermoacoustic instabilities in a premixed combustor," in *29th AIAA Aeroacoustics* Conference, 5–7 May 2008, Vancouver, British Columbia, Canada, p. 2946.

[7]P. Subramanian, S. Marriapan, R. I. Sujith, and P. Wahi, "Bifurcation analysis of thermoacoustic instability in a horizontal Rijke tube," Int. J. Spray Combust. Dyn. **2**, 325–355 (2010).

[8]V. R. Unni, Y. M. Prasaad, N. Ravi, S. M. Iqbal, B. Pesala, and R. Sujith, "Experimental investigation of bifurcations in a thermoacoustic engine," Int. J. Spray Combust. Dyn. **7**, 113–129 (2015).

[9]K. I. Matveev, "Thermoacoustic instabilities in the Rijke tube: Experiments and modeling," Ph.D. thesis, Cal Tech. Pasadena, CA, 2003, pp. 39–72.

[10]K. Matveev and F. Culick, "A study of the transition to instability in a Rijke tube with axial temperature gradient," J. Sound Vib. **264**, 689–706 (2003).

[11]T. C. Lieuwen, "Experimental investigation of limit-cycle oscillations in an unstable gas turbine combustor," J. Propul. Power **18**, 61–67 (2002).

[12]P. Knoop, F. Culick, and E. Zukoski, "Extension of the stability of motions in a combustion chamber by nonlinear active control based on hysteresis," Combust. Sci. Technol. **123**, 363–376 (1997).

[13]N. Noiray and B. Schuermans, "Deterministic quantities characterizing noise driven Hopf bifurcations in gas turbine combustors," Int. J. Nonlinear Mech. **50**, 152–163 (2013).

[14]F. Culick, L. Paparizos, J. Sterling, and V. Burnley, "Combustion noise and combustion instabilities in propulsion systems," in *Combat Aircraft Noise, AGARD Conference Proceedings 512*, Neuilly sur Seine, France (1992), pp. 18–1.

[15]H. H. Chiu and M. Summerfield, "Theory of combustion noise," Acta Astronaut. **1**, 967–984 (1974).

[16]T. Poinsot, K. Hosseini, C. Le Chatelier, S. Candel, and E. Esposito, "An experimental analysis of noise sources in a dump combustor," Prog. Astronaut. Aeronaut. **105**, 333–345 (1986).

[17]T. C. Lieuwen, "Statistical characteristics of pressure oscillations in a premixed combustor," J. Sound Vib. **260**, 3–17 (2003).

[18]T. C. Lieuwen and A. Banaszuk, "Background noise effects on combustor stability," J. Propul. Power **21**, 25–31 (2005).

[19]I. C. Waugh and M. P. Juniper, "Triggering in a thermoacoustic system with stochastic noise," Int. J. Spray Combust. Dyn. **3**, 225–242 (2011).

[20]I. C. Waugh, M. Geuß, and M. Juniper, "Triggering, bypass transition and the effect of noise on a linearly stable thermoacoustic system," Proc. Combust. Inst. **33**, 2945–2952 (2011).

[21]E. A. Gopalakrishnan, J. Tony, E. Sreelekha, and R. I. Sujith, "Stochastic bifurcations in a prototypical thermoacoustic system," Phys. Rev. E **94**, 022203 (2016).

[22]E. A. Gopalakrishnan and R. I. Sujith, "Effect of external noise on the hysteresis characteristics of a thermoacoustic system," J. Fluid Mech. **776**, 334–353 (2015).

[23]R. Steinert, *Effect of Noise on a Model Thermoacoustic System at Its Stability Boundary* (Springer Spektrum, Berlin, Germany, 2016), pp. 15–37.

[24]D. Zhao, "Transient growth of flow disturbances in triggering a Rijke tube combustion instability," Combust. Flame **159**, 2126–2137 (2012).

[25]J. Roberts and P. Spanos, "Stochastic averaging: An approximate method of solving random vibration problems," Int. J. Nonlinear Mech. **21**, 111–134 (1986).

[26]A. Zakharova, T. Vadivasova, V. Anishchenko, A. Koseska, and J. Kurths, "Stochastic bifurcations and coherencelike resonance in a self-sustained bistable noisy oscillator," Phys. Rev. E **81**, 011106 (2010).

[27]G. C. Maling, "Simplified analysis of the Rijke phenomenon," J. Acoust. Soc. Am. **35**, 1058–1060 (1963).

[28]A. P. Dowling and S. R. Stow, "Acoustic analysis of gas turbine combustors," J. Propul. Power **19**, 751–764 (2003).

[29]A. Fichera, C. Losenno, and A. Pagano, "Experimental analysis of thermoacoustic combustion instability," Appl. Energy **70**, 179–191 (2002).

[30]J. Sterling and E. Zukoski, "Nonlinear dynamics of laboratory combustor pressure oscillations," Combust. Sci. Technol. **77**, 225–238 (1991).

[31]K. I. Matveev and F. E. Culick, "A model for combustion instability involving vortex shedding," Combust. Sci. Technol. **175**, 1059–1083 (2003).

[32]E. Boujo, A. Denisov, B. Schuermans, and N. Noiray, "Quantifying acoustic damping using flame chemiluminescence," J. Fluid Mech. **808**, 245–257 (2016).

[33]A. Peracchio and W. Proscia, "Nonlinear heat-release/acoustic model for thermoacoustic instability in lean premixed combustors," in *ASME 1998 International Gas Turbine and Aeroengine Congress and Exhibition*, American Society of Mechanical Engineers, 1998, pp. V003T006A022–V003T006A022.

[34]F. E. C. Culick, V. Burnley, and G. Swenson, "Pulsed instabilities in solid-propellant rockets," J. Propul. Power **11**, 657–665 (1995).

[35]K. I. Matveev and F. E. C. Culick, "A study of the transition to instability in a Rijke tube with axial temperature gradient," J. Sound Vib. **264**, 689–706 (2003).

[36]A. P. Dowling and Y. Mahmoudi, "Combustion noise," Proc. Combust. Inst. **35**, 65–100 (2015).

[37]W. Tao, M. Mazur, M. Huet, and F. Richecoeur, "Indirect combustion noise contributions in a gas turbine model combustor with a choked nozzle," Combust. Sci. Technol. **188**, 793–804 (2016).

[38]L. Kabiraj, A. Saurabh, N. Karimi, A. Sailor, E. Mastorakos, A. P. Dowling, and C. O. Paschereit, "Chaos in an imperfectly premixed model combustor," Chaos **25**, 023101 (2015).

[39]C. F. Silva, M. Merk, T. Komarek, and W. Polifke, "The contribution of intrinsic thermoacoustic feedback to combustion noise and resonances of a confined turbulent premixed flame," Combust. Flame **182**, 269–278 (2017).

[40]S. Li, Q. Li, L. Tang, B. Yang, and J. Fu, "Theoretical and experimental demonstration of minimizing self-excited thermoacoustic oscillations by applying anti-sound technique," Appl. Energy **181**, 399–407 (2016).

[41]N. Noiray, M. Bothien, and B. Schuermans, "Investigation of azimuthal staging concepts in annular gas turbines," Combust. Theory Modell. **15**, 585–606 (2011).

[42]J. G. Lee and D. A. Santavicca, "Experimental diagnostics for the study of combustion instabilities in lean premixed combustors," J. Propul. Power **19**, 735–750 (2003).

[43]P. D. Spanos, P. Cacciola, and J. Redhorse, "Random vibration of SMA systems via Preisach formalism," Nonlinear Dyn. **36**, 405–419 (2004).

[44]V. Salnikov, M. T. Schaub, and R. Lambiotte, "Using higher-order Markov models to reveal flow-based communities in networks," Sci. Rep. **6**, 23194 (2016).

[45]A. Romanelli, "Distribution of chirality in the quantum walk: Markov process and entanglement," Phys. Rev. A **81**, 062349 (2010).

[46]E. Cinlar, *Introduction to Stochastic Processes* (Courier Corporation, Mineola, NY, 2013), pp. 26–35.

[47]K. Imafuku, I. Ohba, and Y. Yamanaka, "Effects of inelastic scattering on tunneling time based on the generalized diffusion process approach," Phys. Rev. A **56**, 1142–1153 (1997).

[48]R. Huang, I. Chavez, K. M. Taute, B. Lukic, S. Jeney, M. G. Raizen, and E.-L. Florin, "Direct observation of the full transition from ballistic to diffusive Brownian motion in a liquid," Nat. Phys. **7**, 576–580 (2011).

[49]T. Schmiedl and U. Seifert, "Optimal finite-time processes in stochastic thermodynamics," Phys. Rev. Lett. **98**, 108301 (2007).

[50]R. L. Honeycutt, "Stochastic Runge−Kutta algorithms. I. White noise," Phys. Rev. A **45**, 600–603 (1992).

[51]J. A. Freund and T. Poschel, *Stochastic Processes in Physics, Chemistry, and Biology* (Springer Science & Business, Berlin, Germany, 2000), pp. 121–159.

[52]P. Clavin, J. S. Kim, and F. A. Williams, "Turbulence-induced noise effects on high-frequency combustion instabilities," Combust. Sci. Technol. **96**, 61–84 (1994).